

Design of Hydrogen Supply Chain Networks for Cross-Regional Distribution

Mingyang Yang, Linlin Liu,* and Jian Du



Cite This: *Ind. Eng. Chem. Res.* 2025, 64, 4498–4515



Read Online

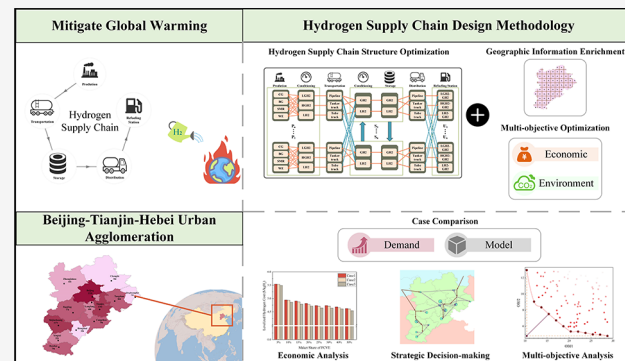
ACCESS |

Metrics & More

Article Recommendations

Supporting Information

ABSTRACT: In the global effort to reduce carbon emissions and mitigate climate change, hydrogen has emerged as a key energy carrier, supporting the transition to a low-carbon economy. This study presents a mixed-integer linear programming model for the design of a cross-regional hydrogen supply chain (HSC), addressing the future challenge of bulk hydrogen distribution. The model aims to make strategic decisions regarding technology selection, facility scaling, construction locations, and distribution methods across different parts of the HSC, encompassing production, storage, transportation, and end-use. The primary goal is to optimize supply chain structures to enhance hydrogen distribution's economic viability and sustainability. The study accounts for hydrogen state transitions during storage and allows distribution among various storage nodes. Additionally, regional grid partitioning is incorporated, integrating geographic data to optimize the layout of hydrogen infrastructure. The model is applied to hydrogen distribution from Inner Mongolia to the Beijing–Tianjin–Hebei Urban Agglomeration, with various scenarios analyzed based on different hydrogen demand forecasts. The results demonstrate that the method proposed in this study can achieve a maximum daily supply chain cost reduction of 2.4%. Furthermore, a multiobjective analysis is performed to balance trade-offs between the leveled cost of hydrogen and carbon emissions. When selecting a compromise solution between the multiobjectives, the economic performance is comparable to that of traditional fuel vehicles, while carbon emissions could be reduced by 26.7%. The resulting insights provide a comprehensive understanding of the interplay between cost-efficiency and environmental impact, guiding strategic decisions for sustainable hydrogen deployment.



1. INTRODUCTION

In 2016, 175 nations endorsed the Paris Agreement,¹ pledging to cap the global temperature increase at 2 °C. By COP 28, the definitive accord called the “UAE Consensus” had been released.² It includes an unprecedented reference to a just, orderly, and equitable transition away from all fossil fuels in energy systems. The growing global demand to reduce greenhouse gas emissions and the search for cleaner fuels have highlighted hydrogen as a potential energy carrier,³ accelerating research into hydrogen energy technologies^{4,5} and the hydrogen supply chain.^{6,7} In China, hydrogen produced from fossil fuels is mainly used in ammonia synthesis, petroleum refining, methanol synthesis, and other chemical processes.⁸ With the introduction of a series of government policies to promote the development of the hydrogen energy industry,⁹ hydrogen has been gradually used as fuel for fuel cell electric vehicles (FCEVs) in China’s energy sector.¹⁰ China’s hydrogen policies primarily focus on the transportation sector. The application of hydrogen fuel cell vehicles and the construction of hydrogen refueling stations have extensively promoted the development of the hydrogen energy industry in many regions.¹¹

However, due to China’s vast territory, there has long been a mismatch in energy supply, necessitating national-level energy regulation measures such as transmission from west to east and mutual support between the north and south grid.¹² This issue similarly applies to hydrogen resources, highlighting the need to establish a cross-regional HSC system for comprehensively managing hydrogen production, transportation, storage, distribution, and application.

The design of the HSC aims to find the optimal configuration, including the location, scale, and process of facilities at each part, as well as the transportation modes between facilities.¹³ Optimizing the HSC for a geographically defined regional scale often utilizes binary and integer variables for configuration decisions. Meanwhile, the hydrogen flow allocation within the supply chain is formulated as a

Received: October 21, 2024

Revised: January 5, 2025

Accepted: January 22, 2025

Published: February 12, 2025



continuous constraint, resulting in the hydrogen supply chain model typically being a MILP.^{14–16} Almansoori et al.¹⁷ were the first to simultaneously consider the processes of hydrogen production, storage, and distribution, designing a MILP model that covers the entire hydrogen supply chain. Subsequently, they extended the model to a multiperiod model,¹⁸ further incorporating the uncertainty of hydrogen demand scenarios across different periods using stochastic programming methods.¹⁹ Kim et al.²⁰ proposed a stochastic model employing a two-stage planning approach that effectively addresses demand uncertainty across various regions. Their work includes a comprehensive multiobjective analysis of HSC,²¹ aiming to optimize economic efficiency and security. Additionally, they developed a multiperiod hydrogen supply system model that incorporates renewable energy sources from different months, facilitating the fulfillment of regional hydrogen demands.²² Subsequent studies have analyzed the hydrogen supply chain design with additional objectives beyond economic feasibility, incorporating considerations such as safety risk,²³ carbon emissions,^{24,25} and multiple environmental indicators.²⁶ There have also been studies simultaneously considering economic, safety risks and carbon emissions,^{27,28} conducting multiobjective optimization research on hydrogen supply chains. Almaraz et al.²⁹ considered these three objectives along with social cost-benefit analysis. Additionally, research has explored the integration of multiperiod and multiobjective optimization for hydrogen supply chains.^{30,31}

Meanwhile, some scholars have refined HSC models to optimize a specific part of the process to improve the economic efficiency of the entire supply chain. Gallardo et al.³² conducted a comprehensive techno-economic analysis of the solar electrolysis process for hydrogen production, applying it to the design of supply chains for the international hydrogen energy trade. Oh, and Niermann et al.^{33,34} regarded liquid organic hydrogen carriers as a safe and efficient hydrogen energy storage and transport method, employing it within the supply chain for energy and economic assessments. Guannan et al.³⁵ explored integrating transportation characteristics of hydrogen transport vehicles and pipelines, incorporating transportation modes and mobile storage capabilities in their model to cater to regional and temporal hydrogen demands. Additionally, some scholars have integrated the HSC model with other complementary models to conduct further research. Dominguez-García et al.³⁶ introduced an optimization approach for the strategic planning of the aviation biofuel supply chain while incorporating the use and production of renewable and fossil hydrogen. Pérez et al.³⁷ developed a mixed integer nonlinear HSC model that included steam methane reforming and carbon capture processes, applying this model to strategic investment decisions related to HSC design and long-term capacity expansion. Li et al.³⁸ integrated the classical HSC design model with the hydrogen fueling station planning, introducing the concept of capturing flows to associate hydrogen demand with origin-destination flows. Some scholars have conducted coupling studies between the HSC and the production processes of hydrogen-based chemical products, including ammonia synthesis,³⁹ methanol synthesis,⁴⁰ and refinery hydrogenation processes.⁴¹ Additionally, researchers have optimized the synergistic planning of hydrogen energy storage and power systems to effectively balance the temporal load variations inherent in hydrogen production processes, thereby reducing carbon emissions.^{42–44}

A few studies also focus on optimizing the topology structure of hydrogen supply chain networks. Seo et al.⁴⁵ developed mathematical models for centralized and decentralized hydrogen storage systems to optimize HSC structures, demonstrating that centralized hydrogen storage methods can effectively integrate dispersed storage regions, resulting in a more cost-effective HSC framework. Similarly, Feng et al.⁴⁶ validated that centralized storage models offer significant economic and environmental advantages during long-term development. Forghani et al.⁴⁷ addressed the multiperiod HSC design problem, proposing a more efficient indirect distribution pipeline transport structure. Hong et al.⁴⁸ conducted detailed techno-enviro-economic analyses of different HSC structures using methylcyclohexane, liquid hydrogen, compressed hydrogen gas, and ammonia as carriers for international energy trade. Wang et al.⁴⁹ proposed a two-layer model to optimize location selection and transportation network systems simultaneously, employing graph theory in the inner layer and a genetic algorithm in the outer layer to address the complex network topology of HSC. In conclusion, existing literature on the design of the HSC primarily focuses on devising supply chain schemes that meet multiple objectives while also accommodating the characteristics of multiperiods. There is considerable attention given to the coupling of various supply chains and the technological selection and optimization of individual segments within the supply chain. However, there is relatively limited research concerning optimizing supply chain network structures.

The network structure of a supply chain consists of a set of nodes (facility location) with different functions and directed line segments (mode of transportation) connecting the nodes.⁵⁰ Optimization of the supply chain structure can be approached by focusing on these two aspects. In optimizing supply chain facility locations, user cities are usually considered sites for building hydrogen infrastructure, while other potential locations within the supply chain region are neglected. To address this issue and achieve a more flexible and diverse supply chain structure, this paper proposes a grid-based division of the supply chain region, incorporating more nodes into the supply chain network structure. To optimize the connections between supply chain nodes, this study considers the interlayer distribution of storage facilities at various locations, utilizing a top-down allocation structure, and allows for phase transformations of hydrogen at these storage sites. The incorporation of these methods provides the supply chain structure design with more diverse hydrogen transportation pathways and a wider selection of nodes, enabling long-term strategic decisions (including the type, location, and capacity of constructed facilities) and the choice of transportation modes at different nodes.

2. HSC MODEL DESCRIPTION

This study proposes a novel superstructure-based mathematical programming model to achieve the optimal design of the cross-regional hydrogen supply chain network. The superstructure comprehensively encompasses the key parts of the supply chain. The phase change during hydrogen storage is considered. Moreover, the hydrogen flow distribution incorporates top-down processes and allows for mutual distribution between storage nodes. By adopting a grid-based approach, more alternative nodes are created to facilitate the optimization of storage locations. The details of the superstructure are presented in the following sections.

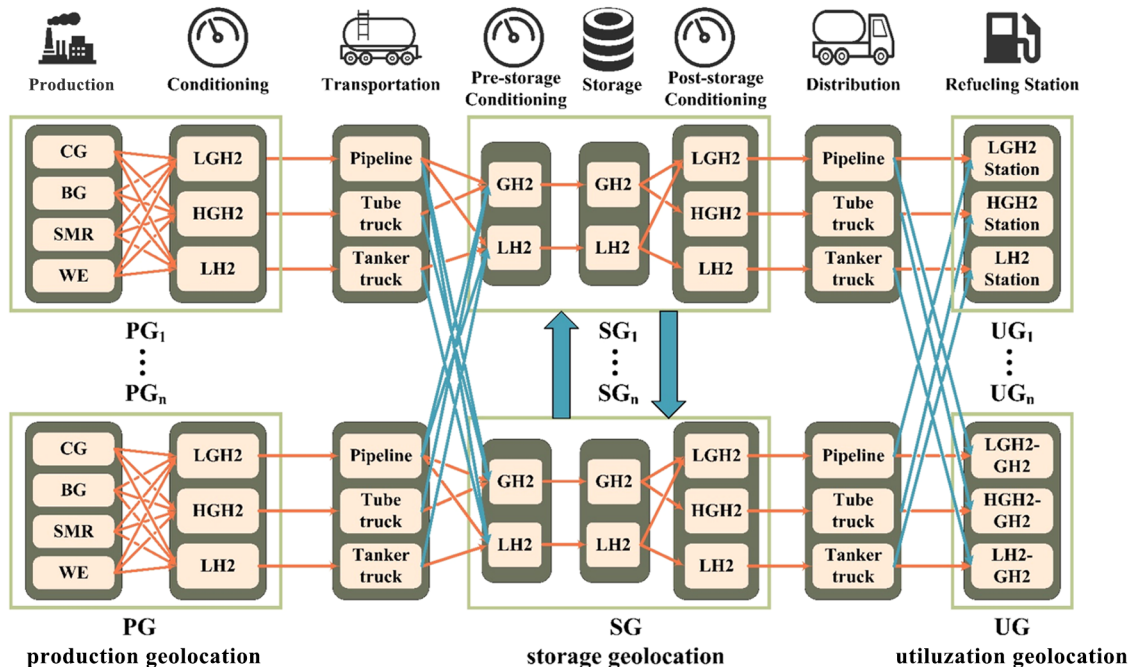


Figure 1. Hydrogen supply chain network superstructure.

2.1. HSC Superstructure. The proposed superstructure is illustrated in Figure 1, composed of the parts of the hydrogen supply chain: production, conditioning, transportation, pre-storage conditioning, storage, post-storage conditioning, distribution, and end-use. The selected hydrogen production processes are technologically mature and widely applied, including steam methane reforming (SMR), coal gasification (CG), biomass gasification (BG), and water electrolysis (WE). Assuming a hydrogen production pressure of 30 bar for all technologies, the hydrogen must be converted into different states depending on the chosen transportation method: low-pressure gaseous hydrogen (LGH2–70 bar), high-pressure gaseous hydrogen (HGH2–250 bar), and liquid hydrogen (LH2). Hydrogen production and conditioning take place at the production geolocation (PG). Pipelines, compressed hydrogen tube trailers, and liquid hydrogen tankers are the candidates for hydrogen transportation. The choice of transportation method depends on the physical state of hydrogen: LGH2 and HGH2 are transported via pipelines and compressed hydrogen tube trailers, respectively, while LH2 is transported using liquid hydrogen tankers.

At the storage geolocation (SG), pre-storage conditioning, storage, and post-storage conditioning of hydrogen occur, as depicted in Figure 1. The hydrogen transported from PG to SG is conditioned and stored in either a gaseous or liquid state, with gaseous storage set at 250 bar. For example, low-pressure hydrogen transported via pipeline is either pressurized or liquefied to meet the storage requirements. Post-storage conditioning is performed depending on the transportation method for the next stage. For instance, stored liquid hydrogen can be gasified for pipeline distribution or loaded into liquid hydrogen tankers for distribution to end-use.

As presented in the superstructure, each HSC configuration is constructed by the stage operations and the pathways that link these operations. It should be noted that the path of liquefying low-pressure hydrogen from pipelines, storing it, and then gasifying it for transportation is not considered, as this

would result in significant energy waste. Such inefficient technical combinations are excluded. The six paths in Table 1

Table 1. Pathways for the Physical State Transformation of Hydrogen

type	transportation type	storage conditioning	storage type	distribution type
type 1	LGH2	compress	GH ₂	LGH2
type 2	LGH2	compress	GH ₂	HGH2
type 3	LGH2	liquefaction	LH ₂	LH2
type 4	HGH2	no phase change	GH ₂	HGH2
type 5	LH2	no phase change	LH ₂	LH2
type 6	LH2	vaporization	LH ₂	LGH2

are established: coupling transportation, pre-storage conditioning, storage, post-storage conditioning, and distribution. The path design is based on the work of SEO.⁴⁵ Compared to the regular single transportation mode, including storage location conditioning processes in the HSC provides a more diversified set of hydrogen transportation pathways for the supply chain network design, enabling decision-making on the transportation mode and conditioning state at different parts.

Hydrogen refueling stations are built at the utilization geolocation (UG). Depending on the distribution method from storage to end-use, the loaded hydrogen must be pressurized or gasified before being injected into the gas cylinders of fuel cell vehicles. The types of hydrogen refueling stations are designated as LGH2-Station, HGH2-Station, and LH2-Station.

2.2. Hydrogen Distribution and Interlayer Mobility. The study divides the HSC into three hierarchical allocation stages from start to end, as illustrated in Figure 2. In the first stage, hydrogen is transferred from the production geolocation to the storage geolocation. The second stage involves intralayer distribution among the storage locations. Finally, in the third stage, hydrogen is distributed from the storage geolocation to the utilization geolocation. This study permits hydrogen

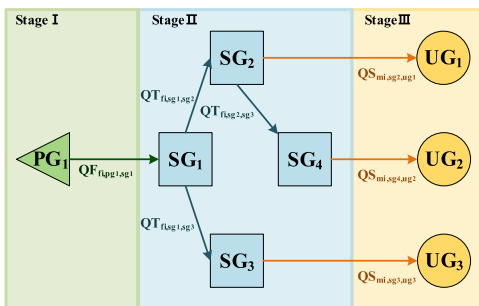


Figure 2. HSC structure incorporates interlayer storage flow.

distribution between intermediate storage nodes during the second allocation stage, a process termed intralayer flow, which has not typically been addressed in prior studies. By integrating this aspect into the system design, it becomes possible to optimize inventory layout and allocate hydrogen flows to meet the varying demand densities across diverse spatial locations effectively.

The distribution process at intermediary nodes can occur in several possible scenarios. As indicated in Figure 2, SG1 distributes hydrogen exclusively to other SGs without supplying any to the end terminals. Hence, no storage facilities are constructed at this node. SG2 allocates hydrogen to both SG4 and the end terminal UG₁, necessitating the construction of storage and storage conditioning facilities to meet the hydrogen demand of UG₁. SG4 solely supplies hydrogen to the end terminal UG₂, requiring the establishment of storage and storage conditioning facilities to satisfy UG₂'s hydrogen demand.

2.3. Geographic Information for Potential Storage Geolocation. Contrary to most hydrogen supply chain designs that identify urban nodes as potential sites for storage facilities, this study divides the supply chain area into a grid based on latitude and longitude,^{51,52} designating the center point of each grid as a potential storage node. This approach increases the number of intermediary node candidates for site selection, offering finer spatial distribution and more flexibility in choosing storage facility locations to supply the entire area effectively. Transportation costs are closely linked to the distances between facilities across different parts of the hydrogen supply chain. The prevailing approach often overlooks the distinction between distances traveled by vehicles and those covered by pipelines, a notable oversight that can affect overall efficiency and cost-effectiveness. To more accurately assess transportation costs, this study utilizes two distinct data sets: driving distances calculated via Baidu Maps' open-source API for truck transportation and pipeline distances derived from the geographical coordinates of locations, calculated using functions from the geopy library in Python.

Accurately determining the transportation distances to hydrogen refueling stations within urban areas poses a significant challenge in the design of hydrogen supply chains. This complexity stems from the intricate urban road networks and varying traffic conditions, making predicting and optimizing transportation routes difficult. An idealized city model is employed for estimation to address this issue.⁵³ This model represents the city as a uniform circular area with hydrogen refueling stations distributed evenly throughout. Accordingly, the distances for pipelines and trucks within the city are calculated using the predetermined formulas eqs 1 and

2 that consider the city's dimensions and the number of refueling stations.⁵³

$$L_{\text{pipeline}} = 2.43 \times N_{\text{stations}}^{0.4909} \quad (1)$$

$$D_{\text{truck}} = 1.44 \times N_{\text{stations}} \quad (2)$$

2.4. Techno-Economic Data. For the effective design of the HSC and the informed making of strategic and tactical decisions, it is critical to thoroughly collect data on production capacity, fixed investment, operational costs, and carbon emissions of technologies available for selection across different parts. Such data should be derived from pertinent literature, research institutions, and government documents. The Supporting Information provides a detailed presentation of the data used in this study.

3. MATHEMATICAL MODEL

A MILP model is established based on the presented superstructure to obtain the optimal supply chain configuration through optimization. This model incorporates mass balance constraints for hydrogen flow allocation, facility capacity, and network structure, along with fixed and operating cost accounting and carbon dioxide emission estimation. The objective function of the single-objective optimization is to minimize the daily cost of the hydrogen supply chain. In the multiobjective analysis, an additional objective function is introduced to minimize the carbon dioxide emissions per unit of hydrogen. The decision variables that should be optimized in the model include the number, technology type, scale, construction location, and production capacity of facilities (including production, storage conditioning, storage, and hydrogen refueling stations) at each part of the HSC as well as the transportation methods and capacities for hydrogen between facilities at different geographical locations.

3.1. Hydrogen Mass Balance Constraints. Equations 3–10 are the hydrogen mass balance constraints for each part of the hydrogen supply chain. At the PG, the processing capacity of the conditioning facility ($CA_{fi,j,pg}$) is equal to the output of the production facility ($PA_{p,j,pg}$), and it is consistent with the quality and physical state of the hydrogen transported to the storage node SG ($HQ_{fi,pj,sg}^F$), as represented by eqs 3 and 4, respectively. Equation 5 presents the hydrogen mass balance at the storage node, where the inflow of hydrogen transported from PG and other SGs equal the sum of the outflow of hydrogen transported to other SGs ($HQ_{fi,xg,sg}^T$) and the processing capacity of the storage conditioning facility ($SCA_{fi,mi,j,sg}$). Equation 6 ensures that the amount of hydrogen processed by the storage conditioning facility is equal to the amount of hydrogen transported from SG to UG ($HQ_{mi,sg,ug}^S$) in both quantity and physical state.

$$\sum_{p \in P} \sum_{j \in J} PA_{p,j,pg} = \sum_{fi \in FI} \sum_{j \in J} CA_{fi,j,pg} \quad \forall pg \in PG \quad (3)$$

$$\sum_{j \in J} CA_{fi,j,pg} = \sum_{sg \in SG} HQ_{fi,pj,sg}^F \quad \forall pg \in PG, fi \in FI \quad (4)$$

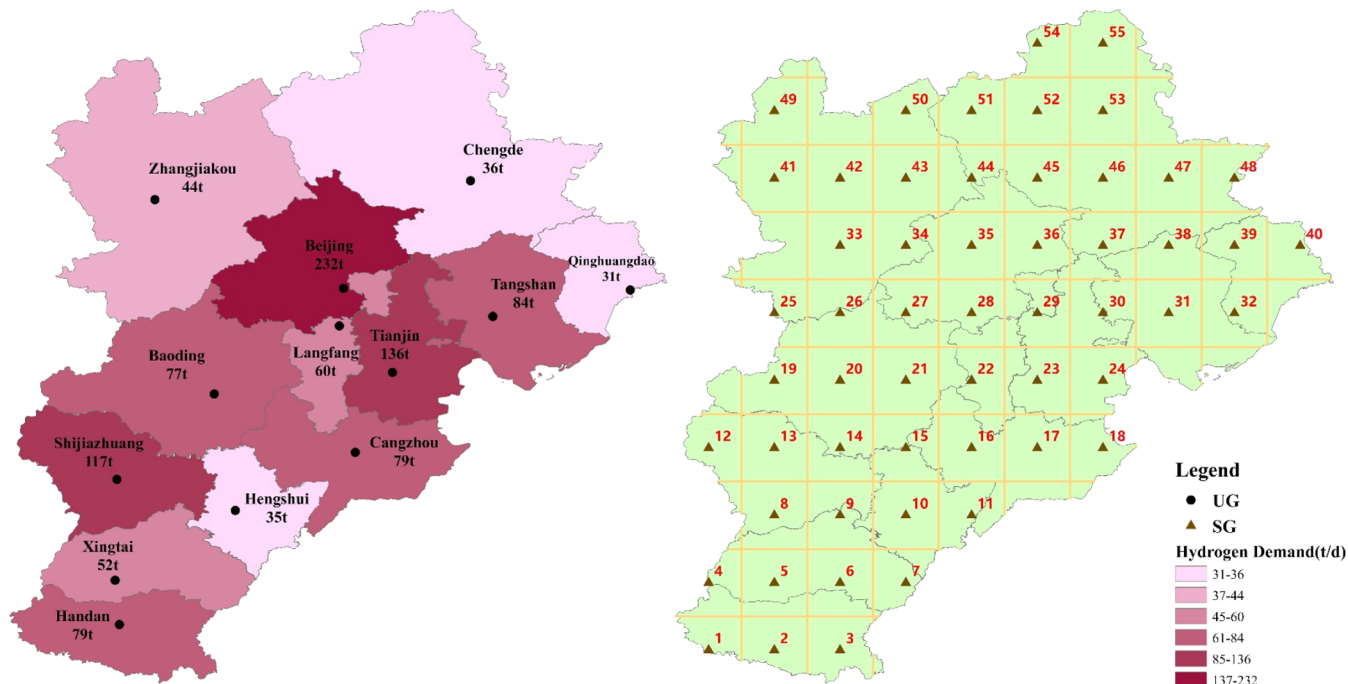


Figure 3. 10% MS hydrogen demand and grid division in the Beijing–Tianjin–Hebei Urban Agglomeration.

$$\text{CRF} = \frac{i \times (1 + i)^n}{(1 + i)^n - 1} \quad (83)$$

$$\text{LCOH} = \frac{\text{TDC}}{\sum_{ug \in UG} \text{DA}_{ug}} \quad (84)$$

In multiobjective optimization, minimizing the carbon emissions per unit of hydrogen is set as an additional objective. The objective function is calculated by summing the carbon dioxide emissions generated during the operation of each part of the hydrogen supply chain and dividing it by the total hydrogen demand across the entire supply chain.

$$\begin{aligned} \min \text{TCO}_2 = & (\text{CO}_2\text{P} + \text{CO}_2\text{C} + \text{CO}_2\text{SC} + \text{CO}_2\text{S} \\ & + \text{CO}_2\text{RS} + \text{CO}_2\text{T}) / \sum_{ug \in UG} \text{DA}_{ug} \end{aligned} \quad (85)$$

3.8. Multiobjective Optimization. This study incorporates the calculation of carbon dioxide emissions within the supply chain design. This enables multiobjective analysis to evaluate the economic and environmental impacts of different supply chain alternatives. Common methods for multiobjective analysis in mathematical programming include the weighting method,⁵⁴ the ϵ -constraint method,⁵⁵ and the augmented ϵ -constraint method.²⁹ When employing the weighting method for multiobjective analysis, different objectives must be assigned weights, though the interpretability of these weights can sometimes be weak. Mavrotas⁵⁶ demonstrated that the augmented ϵ -constraint method exclusively generates efficient solutions, thereby avoiding inefficient outcomes. Govindan et al.⁵⁷ developed a biobjective MILP model for designing a circular closed-loop supply chain network. They compared two constraint methods and highlighted the advantages of the augmented ϵ -constraint method in solving multiobjective optimization problems. Therefore, the augmented ϵ -constraint method is utilized in this study. The model presents the general formulation for solving the multiobjective problem that

incorporates TDC and TCO_2E in eq 86.⁵⁶ In this formulation, eps is defined as a sufficiently small numerical value, typically ranging between 10^{-3} and 10^{-6} . r denotes the difference in carbon emissions between scenarios with the minimum TDC and the minimum CO_2 emissions. e_p refers to numerical points that are evenly spaced within a numerical interval. After eliminating nondominated solutions, the results of multi-objective optimization yield a set of remaining solutions representing all potential designs for the hydrogen supply chain.

$$\begin{aligned} \min & \left(\text{TDC} - \text{eps} \times \frac{s_p}{r} \right) \\ \text{s. t.} & \text{TCO}_2\text{E} + s_p = e_p \\ & s_p \in R^+ \end{aligned} \quad (86)$$

Normalization of the solutions for the two objectives is conducted using the maximum-minimum approach to mitigate the influence of numerical magnitudes. The most suitable design scheme is determined by computing the shortest distance between the ideal point and all solutions,⁵⁸ according to the following eq 87

$$h = \sqrt{(x_s - x_u)^2 + (y_s - y_u)^2} \quad (87)$$

4. CASE STUDY

The case study selected six cities in Inner Mongolia as potential hydrogen production centers based on two primary factors. First, these cities are rich in coal and natural gas resources and wind and photovoltaic resources suitable for hydrogen production.⁵⁹ Additionally, Inner Mongolia has been actively promoting the development of a green hydrogen industrial chain encompassing production, storage, transport, and utilization, supported by its gigawatt-level new energy

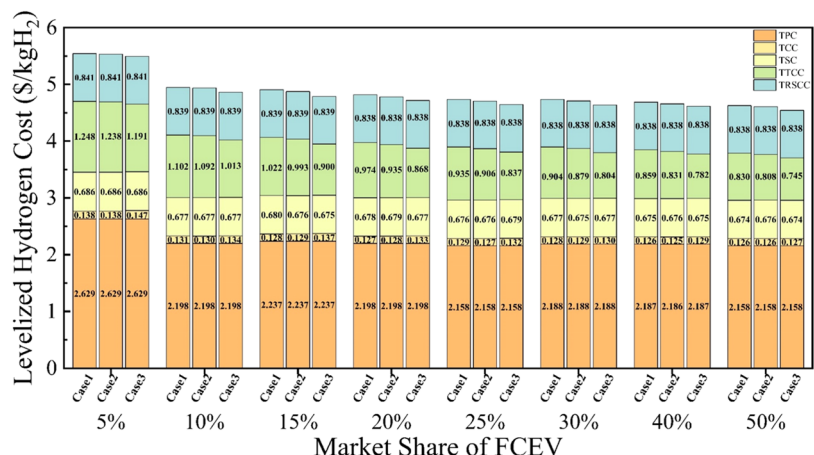


Figure 5. Cost of HSC parts across different market shares.

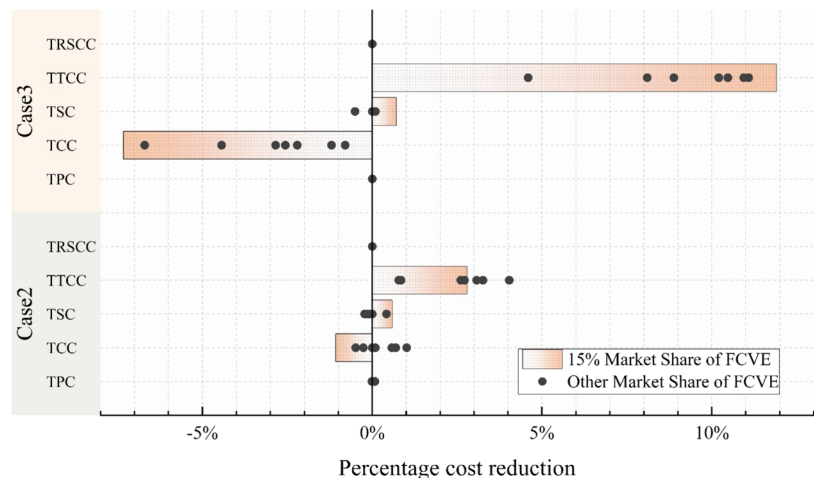


Figure 6. Cost comparison across different parts of the HSC.

hydrogen storage facilities, which are built to accommodate a ten-day supply of hydrogen for end-use, requiring large-scale infrastructure even at lower demand levels. Furthermore, the unit cost of hydrogen at the terminal remains stable because of the small scale and high degree of discreteness of terminal facilities.

Hydrogen production costs exhibit a significant downward trend when market share ranges between 5 and 10%. This is primarily attributed to the centralization effect of production facilities, where initial economic benefits are markedly improved as production scales up. However, as demand continues to grow, the rate of cost reduction gradually slows and fluctuates. During this phase, the design strategy for hydrogen production facilities shifts to a combined model, consisting mainly of large plants supplemented by medium and small plants to meet varying levels of hydrogen demand. It is important to note that the scale and technological choices for hydrogen production remain consistent across the three analyzed cases, leading to minimal differences in unit production cost among them. The same reasoning applies to the consistency in terminal unit hydrogen cost. As shown in Figure 6. Cost comparison across different parts of the HSC, the percentages of hydrogen production and cost reductions converge to zero across different market shares, further supporting this analysis.

5.2. HSC Structure Analysis. This study considers three distinct hydrogen states, each requiring conditioning for transportation, with three corresponding transportation modes. Producing liquid hydrogen involves a complex liquefaction process, which demands high energy consumption and low efficiency, leading to substantial equipment investment and operational costs.⁶² However, it allows for greater loading capacity in liquid hydrogen tanker trucks. In contrast, the decentralized mode of transportation via tube trucks offers lower conditioning costs but comes with reduced loading capacity. As a continuous high-volume transportation option, pipelines have the lowest conditioning cost but require significant fixed investment. The trade-offs between transportation capacity and conditioning cost across these modes necessitate a balanced decision on the final conditioning state and transportation method, focusing on cost optimization.

Table 3 shows the decisions for transportation in stage I, indicating that the pipeline is the primary means of transportation for hydrogen in the three cases. Tube trailers are only used to deliver hydrogen to centralized storage locations in Case 1 and Case 2 when the hydrogen demand is relatively low, at MS at 5 and 10%. As the hydrogen demand grows to 15%, the transportation in stage I is entirely occupied by pipelines. Subsequently, hydrogen undergoes compression and storage before being distributed in stage III using tube trailers. The variation in transportation modes across different

Table 3. Proportional Capacity of Different Modes of Transportation in Stage I

case	market share	tube-truck	pipeline
case 1	5%	0.041	0.959
	10%	0.003	0.997
	other MS	0	1
case 2	5%	0.041	0.959
	other MS	0	1
case 3	other MS	0	1

stages of the HSC topological structure is attributed to the deliberate incorporation of the storage-conditioning. In Case 3, the model incorporates intrastorage node layer flow, enabling the hydrogen distribution among storage nodes via pipelines in stage II. This configuration facilitates centralized pipeline transportation of hydrogen stage I, thereby eliminating the occurrence of modal shifts in transportation. In designing the hydrogen supply chain network, decisions can be made regarding the forms and methods of hydrogen transportation at different stages, allowing for the optimization of cost and avoiding the potential for excessive expenses that might arise from relying on a single distribution pathway.

Further analysis of the cost differences among different cases and their supply chain structures reveals that, at a market share of 15%, Case 2 can save $0.03\text{ $\cdot kgH}_2^{-1}$ cost compared to Case 1. As illustrated in the lower part of Figure 6, the cost differences between the two cases across various market shares are primarily concentrated in the transportation stage, with only minor variations in other parts of the supply chain.

Figures 7 and 8 illustrate the supply chain networks of Case 1 and Case 2. The two networks are quite similar, with

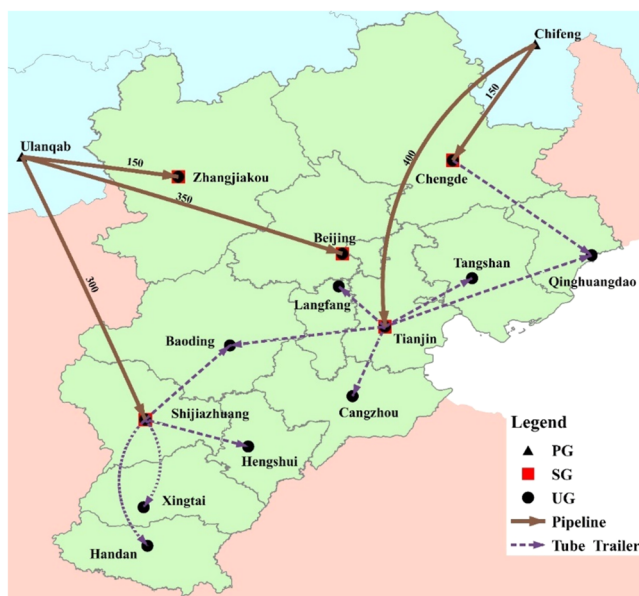


Figure 7. HSC network for Case 1 at 15% market share.

hydrogen being transported from production facilities to storage facilities via pipelines and then distributed to surrounding cities. However, in Case 2, more potential storage nodes are available for selection, enabling the construction of storage facilities closer to areas with higher and more densely distributed demand.

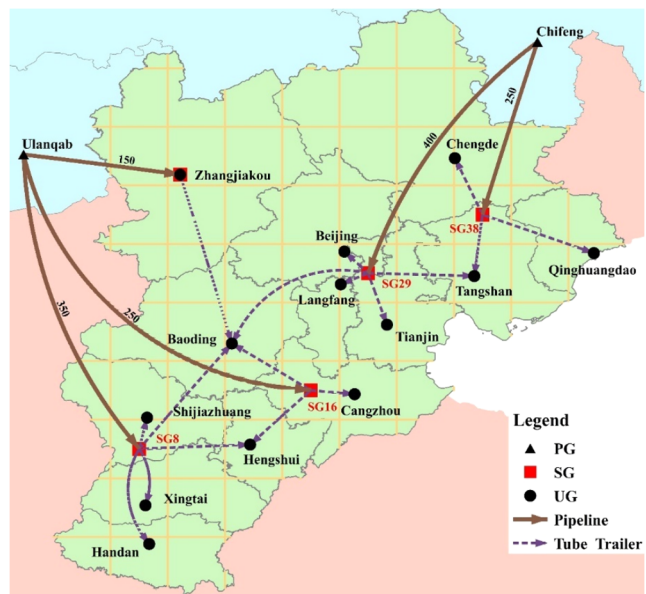


Figure 8. HSC network for Case 2 at 15% market share.

Results for Case 3 indicate potential savings of $0.048\text{ $\cdot kgH}_2^{-1}$ compared to the baseline Case 1, as shown in the upper part of Figure 6. These savings are significant in terms of transportation and conditioning costs, with conditioning costs increasing by up to 7.33%. This increase is due to the more dispersed storage conditioning facilities in the Case 3 structure, as indicated in Figure 9. However, since conditioning cost

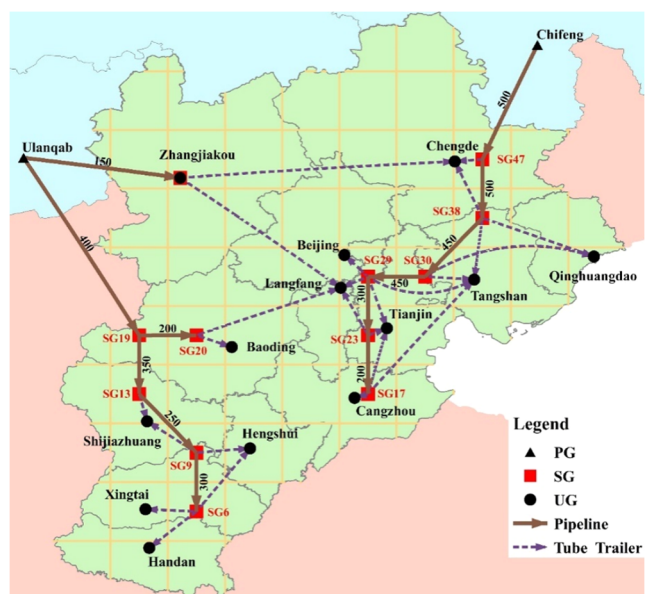


Figure 9. HSC network for Case 3 at 15% market share.

makes up a smaller portion of the overall supply chain cost, this dispersion only results in a modest increase of $0.0094\text{ $\cdot kgH}_2^{-1}$. The most significant cost reduction for Case 3 against Case 1 comes from transportation costs, with an 11.9% decrease, resulting in a cost saving of $0.117\text{ $\cdot kgH}_2^{-1}$. The supply chain diagram in Figure 9 shows that only pipeline distribution is used in stage I. Unlike Case 1, where five pipelines are employed, this case uses three pipelines, forming a branching, tree-like structure. This structure results from

constraints allowing interlayer flow between storage nodes, enabling hydrogen to be distributed from one storage node to another and then to surrounding areas. While this approach requires laying longer pipelines, it creates more storage locations closer to hydrogen demand nodes along the pipeline, reducing the need for multiple pipelines to separate storage nodes. Although this strategy slightly increases transportation costs in stages I and II, it reduces costs in stage III, as does the total transportation cost.

Our findings indicate that, in HSC design, implementing a two-stage (pipeline–tube truck) transportation scheme can enable cost-effective hydrogen distribution. Expressly, hydrogen is initially conveyed over long distances via a tree-structured pipeline network, with storage facilities judiciously positioned based on demand density. Subsequently, tube trucks deliver hydrogen from these storage facilities to terminal nodes, thereby reducing overall distribution expenses. Regardless of the market share occupied by FCEVs, this optimization of node locations and network configuration yields notable economic benefits; in particular, once the market share exceeds 10%, LCOH declines dramatically. This suggests that robust policy support for infrastructure development can hasten the alleviation of high hydrogen costs under low demand and further reinforce hydrogen's competitive advantage over conventional fuels.

5.3. Multiobjective Analysis. Targeting economic minimization, the carbon emissions calculated for the three cases under different hydrogen demands are $28\text{--}29 \text{ kgCO}_2\text{-kgH}_2^{-1}$, which evidently deviates from the original intention of using hydrogen to replace fossil fuels and reduce carbon emissions. To address this issue, the augmented ε -constraint method is employed to perform multiobjective optimization on Case 1 and Case 3, which demonstrated superior economic performance.

The FCEV market share is set at 15% to represent hydrogen demand in the supply chain. The CO_2 emissions calculated when minimizing TDC are utilized as the upper bound for the second objective function. Subsequently, the optimization process is repeated, minimizing the carbon dioxide emissions as the second objective, establishing it as the lower bound. The values between these upper and lower bounds are evenly divided into 11 intervals, each used as constraints, denoted as $e_2\text{--}e_{11}$. The CO_2 emission constraints and multiobjective optimization results for the two cases are shown in Table S12 of the Supporting Information.

As indicated in Figure 10, the Pareto fronts for both cases show a decreasing trend in TDC as carbon dioxide emissions increase, indicating that the two objectives are mutually exclusive. In Figure 11, the Pareto front for Case 3 can be divided into three segments due to varying slopes, indicating a strong correlation with changes in production processes. At point A, to determine the HSC design with the lowest carbon emissions, pipeline distribution is exclusively employed for hydrogen transportation from storage nodes to end-use nodes, and WE is the sole technique used for hydrogen production. Transitioning to point B, stage II transportation shifts entirely to tube trailers, while 15.3% of hydrogen is produced via SMR. The distribution within urban areas via pipelines incurs higher costs compared to using tube trucks, resulting in a smaller decrease in carbon emissions. This explains the steeper slope in segment AB. As carbon emissions constraints increase, segment BC witnesses a transition from electrolytic hydrogen production to predominantly SMR processes, while segment

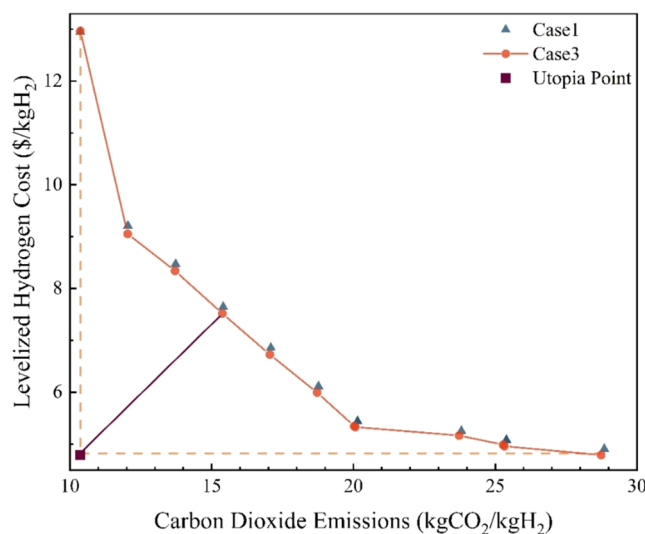


Figure 10. Pareto frontiers of multiobjective optimization.

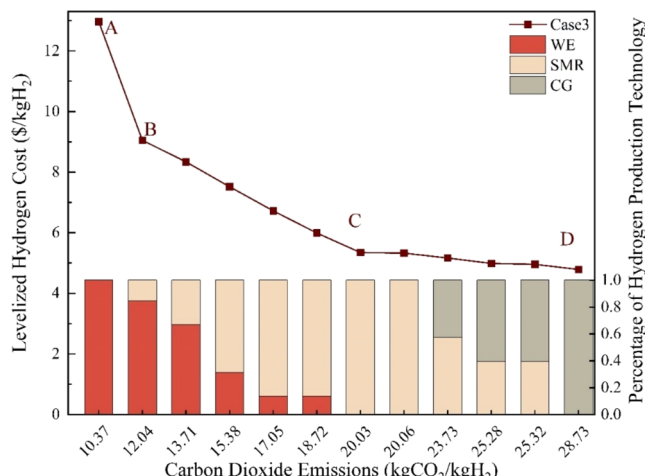


Figure 11. Hydrogen production technology under different carbon constraints.

CD marks a shift from SMR to CG processes. The different slopes in these segments indicate varying cost differentials associated with the three production processes. This demonstrates that reducing carbon emissions in the entire hydrogen supply chain primarily relies on reducing carbon emissions from hydrogen production processes.

Focusing on the Pareto front for Case 3, as shown in Figure 10, it is evident that it lies closer to the ideal point, indicating superior economic and environmental performance compared to Case 1. By normalizing the values of the two objective functions for Case 3 and selecting the shortest distance from the ideal point, GP4 is identified as the final design solution. The hydrogen supply chain structure for GP4, illustrated in Figure 12, primarily differs from the single-objective scenario by transitioning from exclusively using CG processes for hydrogen production to a mix of SMR and WE. The changes in production location selection, processes, and output also lead to variations in the supply chain topology. However, hydrogen is still distributed using a tree-like pipeline from the hydrogen-producing location to the storage location and through tube trucks from the storage location to the end-use.

- (52) Zhang, S.; Liu, L.; Zhang, L.; Zhuang, Y.; Du, J. An Optimization Model for Carbon Capture Utilization and Storage Supply Chain: A Case Study in Northeastern China. *Appl. Energy* **2018**, *231*, 194–206.
- (53) Yang, C.; Ogden, J. Determining the Lowest-Cost Hydrogen Delivery Mode. *Int. J. Hydrogen Energy* **2007**, *32* (2), 268–286.
- (54) Li, M.; Ming, P.; Huo, R.; Mu, H.; Zhang, C. Optimizing Design and Performance Assessment of a Sustainability Hydrogen Supply Chain Network: A Multi-Period Model for China. *Sustainable Cities Soc.* **2023**, *92*, No. 104444.
- (55) De-León Almaraz, S.; Azzaro-Pantel, C.; Montastruc, L.; Domenech, S. Hydrogen Supply Chain Optimization for Deployment Scenarios in the Midi-Pyrénées Region, France. *Int. J. Hydrogen Energy* **2014**, *39* (23), 11831–11845.
- (56) Mavrotas, G. Effective Implementation of the ϵ -Constraint Method in Multi-Objective Mathematical Programming Problems. *Appl. Math. Comput.* **2009**, *213* (2), 455–465.
- (57) Govindan, K.; Salehian, F.; Kian, H.; Hosseini, S. T.; Mina, H. A Location-Inventory-Routing Problem to Design a Circular Closed-Loop Supply Chain Network with Carbon Tax Policy for Achieving Circular Economy: An Augmented Epsilon-Constraint Approach. *Int. J. Prod. Econ.* **2023**, *257*, No. 108771.
- (58) Erdogan, A.; Geçici, E.; Güler, M. G. Design of a Future Hydrogen Supply Chain: A Multi-Objective Model for Turkey. *Int. J. Hydrogen Energy* **2023**, *48* (31), 11775–11789.
- (59) Liu, W.; Hu, W.; Lund, H.; Chen, Z. Electric Vehicles and Large-Scale Integration of Wind Power – The Case of Inner Mongolia in China. *Appl. Energy* **2013**, *104*, 445–456.
- (60) Zhang, W.; Geng, X.; Cheng, S.; Zhou, Q.; Liu, Y. Simultaneous Evaluation of Criteria and Alternatives Method-Based Site Selection for Solar Hydrogen Production Plant in Inner Mongolia, China. *Sustainable Energy Technol. Assess.* **2024**, *61*, No. 103583.
- (61) Zhang, Q.; Chen, W.; Ling, W. Policy Optimization of Hydrogen Energy Industry Considering Government Policy Preference in China. *Sustainable Prod. Consumption* **2022**, *33*, 890–902.
- (62) Zhang, T.; Uratani, J.; Huang, Y.; Xu, L.; Griffiths, S.; Ding, Y. Hydrogen Liquefaction and Storage: Recent Progress and Perspectives. *Renewable Sustainable Energy Rev.* **2023**, *176*, No. 113204.
- (63) Heidary, H.; El-Kharouf, A.; Steinberger-Wilckens, R.; Bozorgmehr, S.; Salimi, M.; Golmohammad, M. Life Cycle Assessment of Solid Oxide Fuel Cell Vehicles in a Natural Gas Producing Country; Comparison with Proton Electrolyte Fuel Cell, Battery and Gasoline Vehicles. *Sustainable Energy Technol. Assess.* **2023**, *59*, No. 103396.
- (64) Chen, Y.; Melaina, M. Model-Based Techno-Economic Evaluation of Fuel Cell Vehicles Considering Technology Uncertainties. *Transp. Res. D: Transp. Environ.* **2019**, *74*, 234–244.